Understanding Role of Flow Obstacle on Bubble Behavior and CHF in Two-Phase Boundary Layer Flow

U. Jeong and S. J. Kim*
Department of Nuclear Engineering, Hanyang Univ., 222 Wangsimni-ro, Seongdong-gu, Seoul 04763, Republic of Korea
**Corresponding author: sungjkim@hanyang.ac.kr*

1. Introduction

In South Korea, a design of an ex-vessel corium cooling system using an external core catcher has been proposed as one of the severe accident mitigation measures for the requirement of European Utility Requirements (EUR). A key design component of the core catcher system is the engineered corium cooling system, where the decay heat generated from the molten corium is removed by the boiling of water. The cooling system consists of a cooling channel amid the corium spreading compartment and inside wall of the cavity. Many short columnar structures, called stud, are placed at the cooling channel to support the static and dynamic loadings on the core catcher body and to provide coolant flow paths underneath the core catcher body. As shown in Fig. 1, the cooling channel consists of a vertical channel and a 10° inclined channel, which are designed to facilitate bubble venting. The slightly inclined channel, where studs are installed, is of interest in the present study.

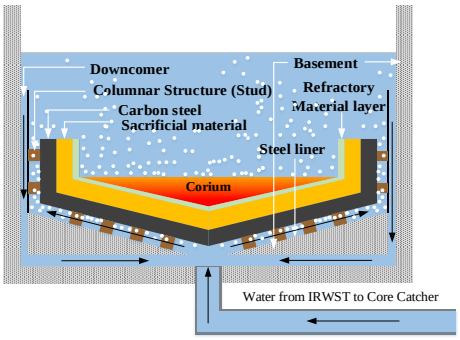

Fig. 1. Conceptual design of the ex-vessel core catcher system with boiling induced two-phase natural circulation under the ex-vessel phase of severe accident.

The following key thermal hydraulic features unique to the cooling channel have drawn critical attention with respect to the CHF.

- Slightly inclined flat and large heater surface facing downward
- Low flow in boiling induced natural circulation
- Low pressure and a large hydraulic diameter
- High thermal inertia of the thick heater surface resistant to premature CHF due to frequent formation of dry-patch
- Many aligned columnar structures installed in the cooling channel

For the case in which boiling occurs on a downward facing heater surface, if the heated area is sufficiently large, a stable two-phase boundary layer flow can appear along the heater surface even under fairly low heat flux level. The presence of the two-phase boundary layer flow may affect the two-phase structure near the heater surface.

Owing to the stud, significant flow blockage and corresponding distortion of the streamline are unavoidable. Possible flow stagnation in the region between studs may lead to accumulation of bubbles at the stagnant region. Thus, the aligned studs would play a role of an obstacle and confine the bubbles in the region. Yang et al. [1] reported that, for downward facing plates, the increase in difficulty of bubble escape from the heater surface can lead to a CHF decrease, implying a negative influence of the studs on the CHF.

On the other hand, prior studies on flow boiling with obstacle showed that the obstacle, such as rod-spacing devices, can produce a large enhancement of the CHF. Pioro et al. concluded that the presence of flow obstacles in a flow channel delayed the CHF through an increased turbulent intensity. However, it was observed that the obstacles were ineffective enhancing the CHF and even decreased the CHF at low mass fluxes and qualities.

As analyzed above, previous studies could not show clearly if flow obstacles certainly had positive effects on the CHF. Thus, investigating the effects of flow obstacles on the CHF is considered important if an optimal design of the ex-vessel core catcher cooling system is to be determined. The aim of this study was to obtain CHF data with various obstacle shapes and mass flow rates to find an optimal geometry of the columnar structures in the cooling channel. To achieve the objective, a laboratory-scale test section was designed, considering the aforementioned key thermal-hydraulic features of the prototypical core catcher cooling system.

2. Experimental Apparatus

2.1 Test section assembly

In the test section design, as a key similarity criterion in the down-scaling process, a stable formation of two-phase boundary layer flow was chosen owing to its influential impact on the liquid supply and bubble escaping processes. For a successful simulation of the thermal-hydraulic phenomena, geometric dimensions for

the test section as well as the heating method were determined carefully.

The characteristic length of a stud was determined to simulate the physical phenomenon, in which a sufficiently small momentum transfer exists between the bubbles moving in the obstacle-free region and the bubbles departing from the stagnant region between the studs. Accordingly, heater length, width, and a distance between the adjacent studs were determined as 216 mm, 108.5 mm, and 107.5 mm, respectively. Channel height was also determined to be 30 mm to sufficiently minimize the direct interaction between the bubble and the unheated wall. Figure 2 shows the test section assembly. To calculate the heat flux, vertically aligned three K-type thermocouples (0.5 mm dia.), each spaced 10 mm apart, were inserted into the heating block to measure the temperature gradient.

In this study, several stud shapes, square with dimensions of 25 × 25 × 30 (height) mm^3, circular with a diameter of 28.2 mm, elliptic with dimensions of 37 mm (major axis) and 21.6 mm (minor axis), were tested. Figure 2 presents the arrangement of the studs as well as the detailed view of the test section.

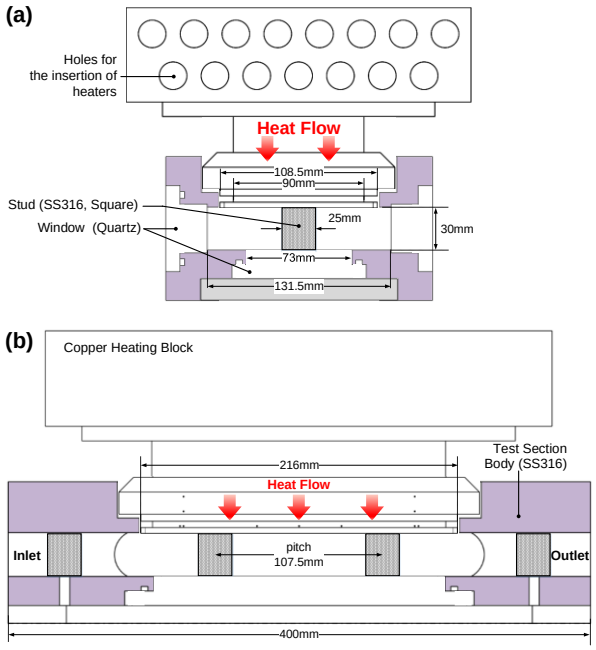

Fig. 2. Sectional views of the test section in which stud structures are installed.

2.2 Boiling loop with instrumentation system

The water boiling loop is shown in Fig. 3. An optical fiber microprobe, with diameter of 125 μm, was used to measure the vapor fraction at the tip of the probe and to provide information about the two-phase flow structure in the vicinity of the heater surface optically blocked by stratified bubbles near the heating surface.

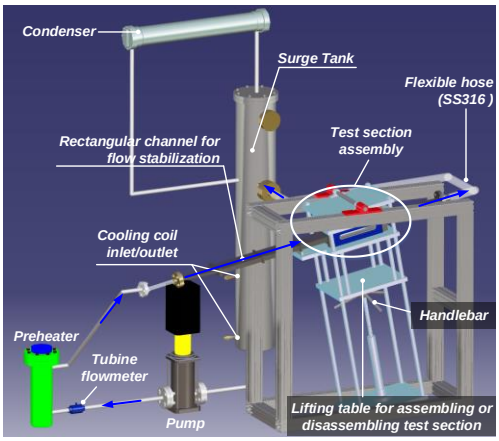

Fig. 3. 3D drawing of the forced convective water boiling loop.

2.3 Experimental procedure and uncertainty

In the present experiments, the heater surface could be regarded as a "fresh" surface in every experiment as hydrochloric acid (35wt %) was used to remove the contaminant deposited on the heater surface during the last boiling experiment. In all the experiments, the absolute pressure at the outlet and inlet subcooling were maintained at 1.07 bar and 5 K, respectively.

The calculated relative uncertainty of the heat flux, which is a function of heat flux and the uncertainty, continuously decreases from 16% to 5% with the change in heat flux from 100 to 400 kW/m2. In other words, the relative uncertainty is calculated to be less than 5% at elevated heat fluxes above 400 kW/m2, beyond which CHF would occur in this study

3. Results and Discussion

The local heat flux was used to measure the CHF value, at which a sudden and continuous rise in the surface temperature beyond 200℃ appears simultaneously with an abrupt decrease in the local heat flux, following an incremental increase in the heater power.

3.1 Dependence of CHF on the mass flow rate

The relation between the mass flux and CHF was examined in the test section where studs were not installed. The results, shown in Fig. 4, present CHF variation with mass flux, and predicted CHF values from the existing pool boiling CHF models.

A linear proportional relation was confirmed. Existence of the transition mass flux may be attributed to the delayed transition in flow pattern and a corresponding change in the contribution of turbulent motion to the liquid supply on the heater surface. This analysis is supported by Oyewole's work (2013) and the present experimental data of local void fraction traces.

Importance of phase distribution near the heater surface on CHF could be emphasized well through the analysis.

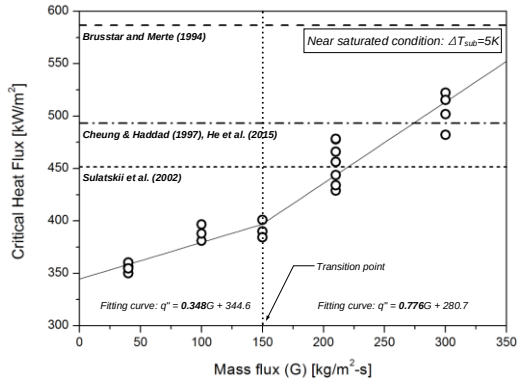

Fig. 4. Dependence of CHF on the mass flux under near saturated condition.

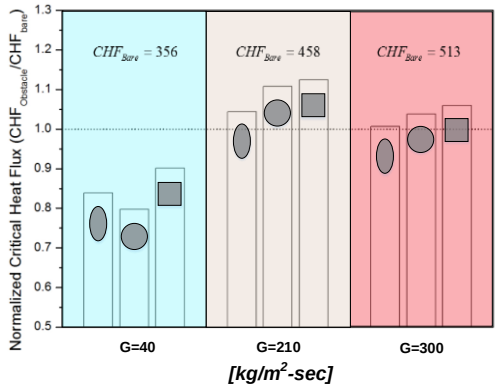

Fig. 5. Influence of stud shape on CHF with variation in mass flux.

3.2 Influence of the aligned flow obstacles on CHF

Figure 5 presents the CHF data normalized by the CHF in the bare case. When flow obstacles are absent in the channel, the abrupt temperature excursion owing to occurrence of the CHF commonly takes place at the downstream of the heater surface first. In the channel with the aligned flow obstacles, however, the CHF occurred at the stagnant region between the obstacles, especially right after the upstream obstacle. The aligned obstacles imposed a positive effect on the CHF enhancement irrespective of the obstacle shape when the mass flux was over 200 kg/m^2-s. It should be noted that the elliptical shape showed the poorest performance with respect to the CHF even though the elliptical shape obviously provides the best hydrodynamic advantages of a smooth curve and the lowest blockage ratio. This result gives us an important insight about the CHF triggering mechanism, that is, hydrodynamic advantages of ellipses do not necessarily guarantee efficient bubble venting compared to those of other shapes.

The negative effect of the aligned flow obstacles, irrespective of the stud shape, on the CHF was observed under a mass flux condition of 40 kg/m2-s, at which the bubble dynamics is similar to that in the pool boiling condition.

The positive influences of obstacle are closely related to the phenomena of disintegration of bubbles and an oscillating vortex shedding flow, and resultant easier liquid supply to the heater surface. Note that the phenomena are correlated with each other. Several possible mechanisms of disintegration of a bubble were described in Ref. [2]: abrupt acceleration of liquid, influence of stresses on a bubble in the gradient field, effect of turbulent pulsations, and development of instability of the interface boundary. It can be deduced that the abovementioned mechanisms would be implemented actively through the collision process between moving fluid and obstacle. Fig. 6 presents the bubble disintegration phenomenon induced by the collision.

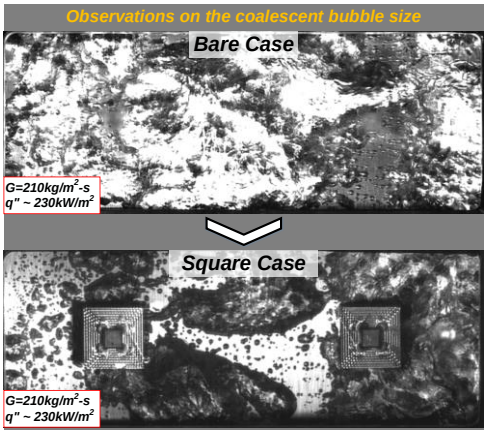

Fig. 6. Visual observations on the bubble disintegration.

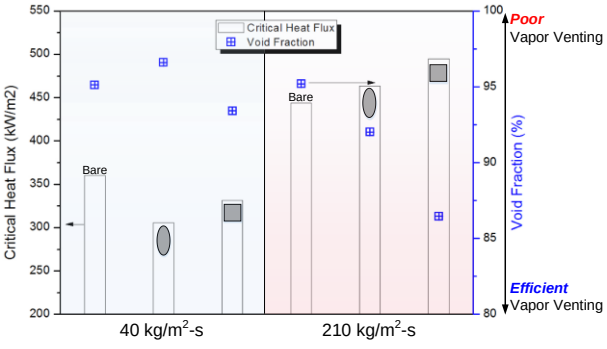

Fig. 7. CHF and local void fraction with variation in mass flux, obstacle shape.

Right before the CHF occurred, the local void fraction was measured at a location near the position at which CHF. At a low mass flux condition, the flow obstacles could not make a significant deviation in void fraction from that of bare case. However, at a high mass flux condition, it was shown that a lower void fraction was measured despite the existence of obstacles compared to the bare case. Here, it should be noted that even though higher heat flux is needed to for the boiling

crisis caused by the flow obstacles to occur, the corresponding local void fraction decreases. That is, the vapor venting process is considerably enhanced owing to the flow obstacles, and depends highly on shape of the flow obstacle. Noticeable reduction in the void fraction was observed in the case of the square shaped obstacle when compared to the ellipse case. These results can be explained by investigating obstacle-induced change in hydrodynamics in the channel. This will be covered in the next section by using a CFD tool, ANSYS FLUENT.

3.3 CFD analysis

Only liquid phase (saturated water) was modeled in the simulation to avoid unnecessary complexity. Experimental observation of a stratified two-phase flow supports the hypothesis that the single phase simulation used in this study would provide adequate results on the general tendency of the bulk flow characteristics in the channel.

In the modeling of turbulence, a detached eddy simulation was used to capture instantaneous turbulent motion, which cannot be captured by RANS based models. In fact, 3D simulation is most suitable for turbulence modeling considering the random nature of turbulence. However, 2D analysis was used to reduce computing resources, considering the required simulation time of 10 s. Such a long simulation time arises from the long evolution time required for the obstacle induced wake turbulence be fully developed.

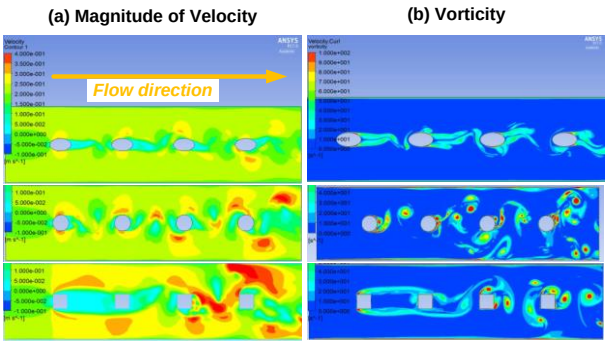

Fig. 8. Representative contours; (a) velocity, (b) vorticity.

In the case of square and circular shaped obstacles, it was observed that flow with high velocity crosses the stagnant region between the obstacles repetitively as seen in Fig. 8. From the contours of vorticity (See Fig. 8(b)), we could observe a remarkable oscillating flow, called vortex shedding, only in case of the square and circular shaped obstacle. This result revealed that the obstacle induced oscillating vortex shedding creates cross flow with high velocity over the stagnant region. The increased velocity in the stagnant region due to the cross flow raises the shear lift force exerted on the bubble, facilitating bubble detachment process. Furthermore, the vortices themselves raise the shear lift force. Because of cross flow, at the same time, the detached bubbles are swept away to the obstacle-free flow region where bubbles are vented expeditiously.

In that way, the flow obstacle can be favorably regarded with respect to the vapor venting process at an inlet velocity of 0.2 m/s, except for the ellipse case. By observing the bubble behavior with help of the high-speed camera, bubble dynamics involved in the enhanced vapor venting process due to the obstacle are observed, and they are presented schematically in Fig. 9.

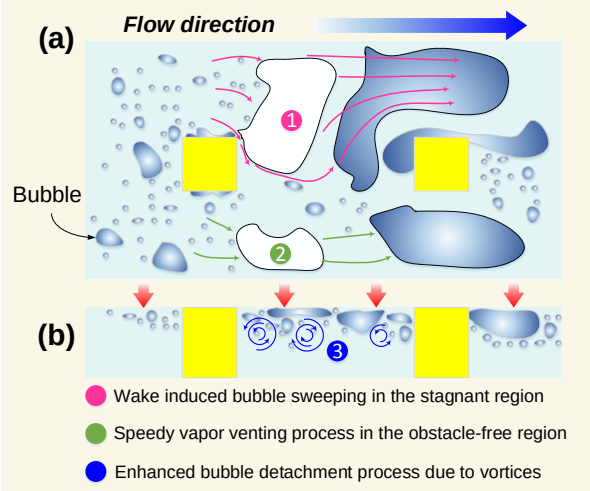

Fig. 9. Bubble dynamics involved in the enhanced vapor venting process owing to the obstacle induced wake.

4. Conclusions

The key physical mechanisms through which the aligned obstacles affect the CHF were confirmed as the disintegration of a large bubble and repeating turbulent wake-induced enhancement in the bubble detachment process and bubble sweeping in the stagnant region.

Near the saturated water condition, positive influence of the columnar structures in the cooling channel has been clarified with respect to the CHF, considering that a reported natural circulation flow rate exceeds 200 kg/m^2-s .

ACKNOWLEDGEMENTS

This work was supported by the National Research Foundation of Korea (NRF) grant funded by the Korea government (MSIT) (Nos. 2017M2B2A9A02049735 and 2017M2A8A5018575)

REFERENCES

[1] S. H. Yang, W. P. Baek, and S. H. Chang, Pool-boiling critical heat flux of water on small plates: effects of surface orientation and size, International communications in heat and mass transfer, Vol. 24, p. 1093-1102, 1997.

[2] A. Avdeev, Bubble systems: Bubble Breakup, Springer International Publishing, Switzerland, 2016.